

Finite Element Analysis and Experiments on a Dual Stator Winding Brushless Alternator (DSWBA) Suitable for Remote Isolated Areas

M. El-Shanawany, S.M.R. Tahoun and M. Ezzat
Electrical Engineering Department
Faculty of Engineering
Menoufia University

Abstract- This paper presents the performance and design of 1.6 KVA, through finite element, dual stator winding brushless alternator suitable. The proposed generator is suitable for operation at high speed since it has a brushless construction. It also has a rigid construction whereas its rotor has neither windings nor a permanent magnet. In this design there are two sets of windings to be embedded in the stator slots. One, referred to as multi-phase power winding, supplies power to the load. The other winding, called the excitation winding which is connected directly to a dc supply. Different from the brushless synchronous generator, there is no need for the built in diodes in the rotor circuit. A prototype was built to verify the proposed design and to investigate its performance.

Index Terms- Alternator, Brushless, Design, Dual Stator Winding

I. INTRODUCTION

Recently, interest in dual stator windings [1] and brushless doubly fed motors to be used in adjustable speed drives (ASD's) has been revived [3-6]. The brushless doubly fed machine (BDFM) allows the use of partially rated inverter and represents an attractive cost-effective candidate for variable speed applications with limited speed ranges. Brushless doubly fed induction motors (BDFIM's) have significant rotor losses and poor efficiency. The reluctance version of BDFM's which known as brushless doubly fed reluctance motors (BDFRM's) [3-11] have no rotor windings and therefore no rotor copper losses which offer the prospect for higher efficiency. On the other side synchronous generator has great advantages but suffers from brushes and slip rings existence in its rotor that increases the need for maintenance and therefore reliability reduction. The brushless version of synchronous generator has no brushes and slip rings but it uses built in diodes and extra foundations. To avoid the need for these diodes and the extra foundations in brushless synchronous generator, both field and generating windings must lie in the stator and must be coupled sinusoidally. These requirements can be achieved by using the principle of operation and the same construction of DFRM's.

II. MACHINE CONSTRUCTION

Construction of the proposed generator is the same construction as the BDFRM. It consists of stator and rotor. The stator is made from silicon steel laminations in the same way of induction machine stator. As shown from Fig. 1, dual sets of three-phase windings with different pole numbers are placed in the slots (2 and 6 are chosen in this paper), in the same manner as in the self-cascaded induction machine[12].

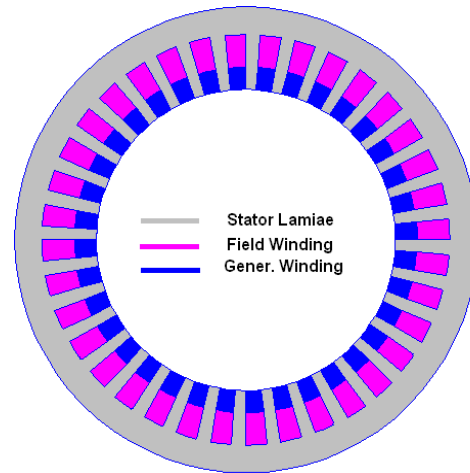


Fig. 1 DSWBA Stator and Winding Arrangement

One of the dual stator winding acts as a "generating" or "power" winding and can be connected star or delta. The other winding acts as a "field" winding and is excited from a DC power supply. Field phases can be connected in several manners. They can be connected as open delta with two reversed phases (ODWTRP) or parallel connected with two reversed phases (PCTRP) or two phases in parallel in series opposition with the third phase (TPPSTP). Fig. 2 shows the used connections. The first connection is the most suitable one and is used in this paper. Different from the self cascaded induction machine, the rotor of the proposed generator is of the reluctance type (A flux barrier type was designed and chosen in this paper).

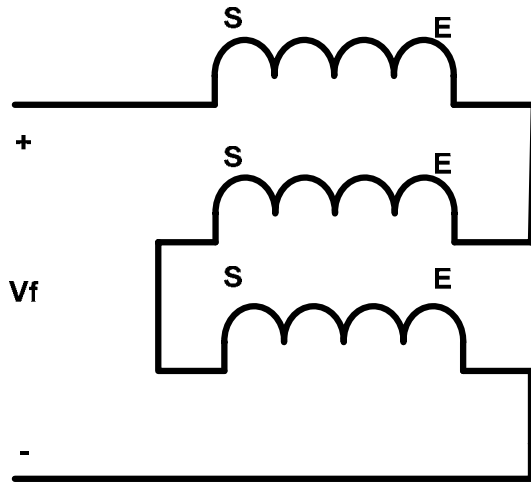
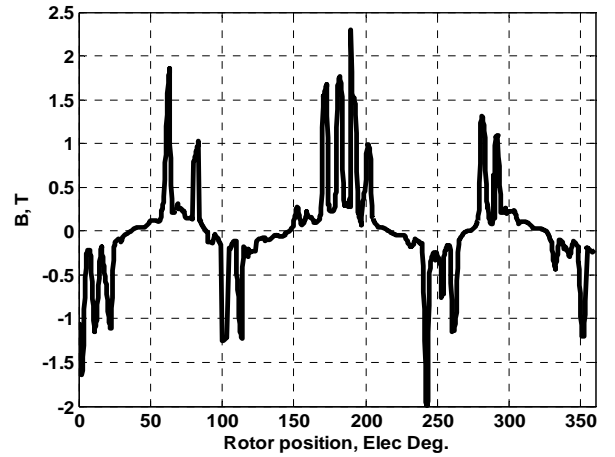


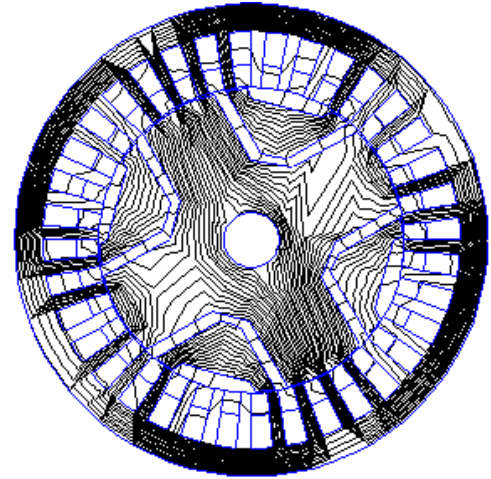
Fig. 2 ODWTRP Connection

III. THEORY OF OPERATION

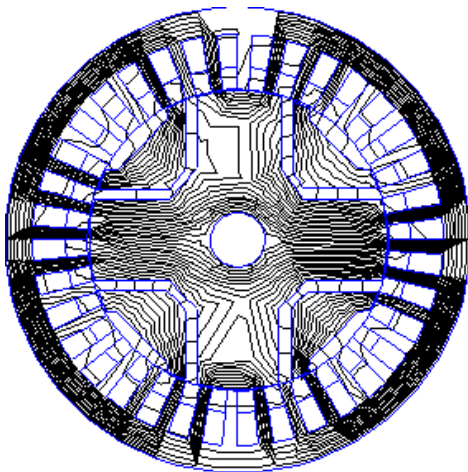
For clearance, a finite element tool was used to show the variation of magnetic field density in the air gap with rotor rotation. It was applied on a machine of four rotor poles with a stator of 36 slots carrying two sets of 3-phase windings with six and two poles. Figs. 3&4 show the variation of air gap flux density at two rotor positions. From these figures we can find that with rotor rotation, there is a variation in flux density and certainly in flux which means there is a change in flux linking generating winding with time. Therefore, a voltage will be induced in generating windings. The induced voltages in generating winding phases will be shifted by 120 electrical degrees from each others as a result 120 electrical degrees shift between each phase.



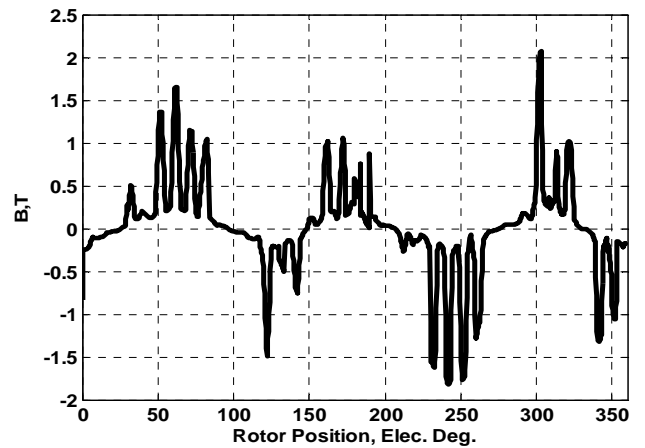
b. Air Gap Flux Density Distribution (At $\theta=0^\circ$)
Fig. 3



a. Flux Distribution (At $\theta=60^\circ$)



a. Flux Distribution (At $\theta=0^\circ$)



b. Air Gap Flux Density Distribution (At $\theta=60^\circ$)
Fig. 4

IV. EMF EQUATION

Fig. 5 gives the variation of magnetic flux linking a generating winding phase and its two components with rotor angular position. There is no induced voltages result from the DC component, but the AC component produces induced voltages with rotor rotation.

The magnetic flux linking a generating winding phase can be expressed as follows:

$$\varphi(t) = \varphi_1 + \varphi_2 \cos(p_r \omega_{rm} t) \quad (1)$$

From finite element analysis, φ_2 is found to be equal to φ_{pm}/π and the rms induced voltage is found to be:

$$E_{rms} = 4.44 f W_{ph} K_w \varphi_{pm} / \pi \quad (2)$$

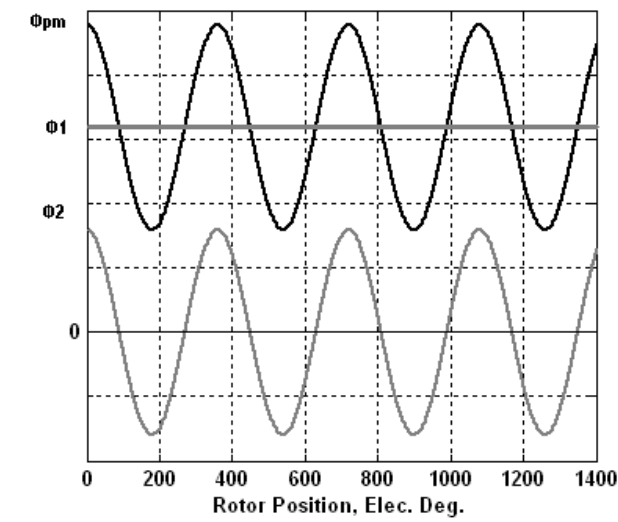


Fig. 5 Flux Variation and its Components

V. PROPOSED GENERATOR DESIGN

The starting point in rotating machine design is to calculate machine main dimension. Main dimensions of DSWBA can be calculated from an output equation as follows:

$$S_n = 3 E_{rms} I_{ph} * 10^{-3} \text{ KVA} \quad (3)$$

Substituting from equation (2) into equation (3), output equation is found to be:

$$S_n = C_o D^2 L n_s \quad (4)$$

Where:

$$C_o = (2.22) \gamma \pi * ac * K_w * 10^{-3}$$

From the above equation, it can be shown that the output equation of the DSWBA is similar to the output equation of the conventional synchronous generator except the output coefficient (C_o).

For the same ampere conductor (ac), same speed (n_s), same axial length (L), same air gap length and the same nominal power (S_n), it is found that the bore diameter of the DSWRG is

approximately doubled. Number of field conductors per slot with double field current used in this design is calculated from:

$$Z_f = \frac{2 W_f P_r}{s K_{wf}} \quad (5)$$

Where:

$$K_{wf} = \frac{\sin \frac{q'' \alpha}{2}}{q'' \frac{\alpha}{2}} \quad (6)$$

$$q'' = \frac{s}{2 p_2} \quad (7)$$

$$\alpha = \frac{360}{s} * p_2 \quad (8)$$

VI. TEST RIG

The stator of 36 slots of a 1 hp three-phase induction motor is modified to fit the nature of the DSWBA by replacing the original winding by two sets of three-phase windings having different number of poles. One of these windings has 6-pole and is used as a field winding by connecting its phases in series with two reversed phases. The other winding has 2-pole and used as a three-phase generating winding. Fig. 6 shows a photo of the stator of the proposed DSWBA. Instead of induction motor rotor a flux barrier rotor (4 poles) is used. Fig. 7 shows photo of this rotor. Table 1 gives the design data of the used rotor.



Fig. 6 Prototype Stator



Fig. 7 Flux Barrier Rotor

Flux Barrier Rotor	
Radial rib	1 mm
Tangential rib	1 mm
Barrier width	6mm
Cut_out depth	7 mm

Table 1 Flux Barrier Rotor Design Data

VII. EMF VERIFICATION AND PERFORMANCE

Fig. 8 gives the no load characteristics of the experimental generator with the flux barrier rotor. There is a good agreement between the experimental and the calculated result which ensures equation (2) and so the proposed design.

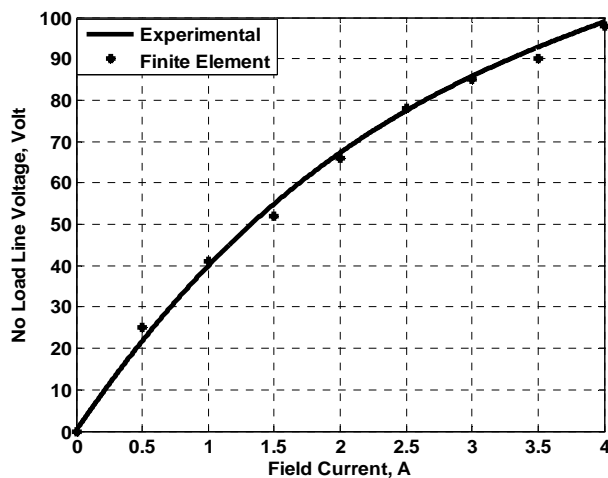


Fig. 8 No Load Characteristics at 1500 R.P.M.

Fig. 9 show the generated voltage per phase at no load. As seen from this figure, the waveform contains harmonics. It is expected that the voltage waveform will approach to the sinusoidal waveform with loading. Also, the use of laminated rotor and pole skewing may reduce the harmonic content.

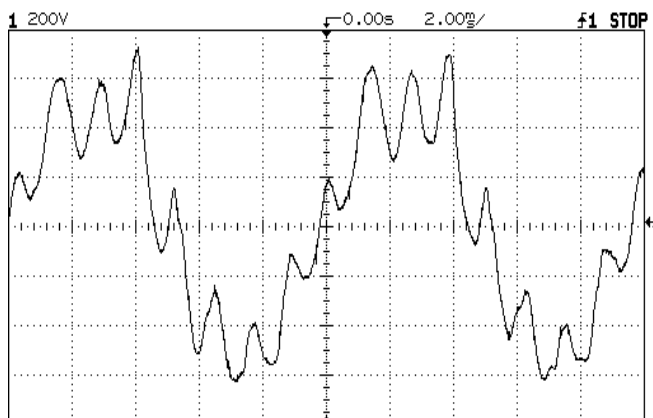


Fig. 9 No Load Per Phase Voltage ($I_f=2A$, 1500 r.p.m., voltage Scale=10:1)

Fig. 10 shows the waveforms of phase terminal voltage and phase current with R-load. As expected before, the waveforms approach from sinusoidal waveform with loading.

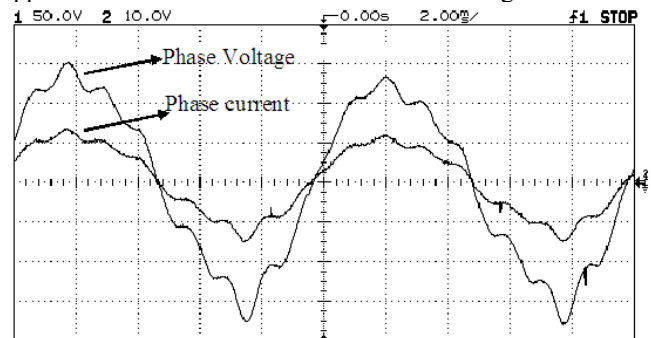


Fig. 10 Terminal Per Phase Voltage & phase Current ($I_f=2A$, 1500 r.p.m., voltage Scale=10:1)

Fig. 11 shows the terminal voltage per phase for two phases for field current (I_f) of 2A and at 1500 r.p.m.

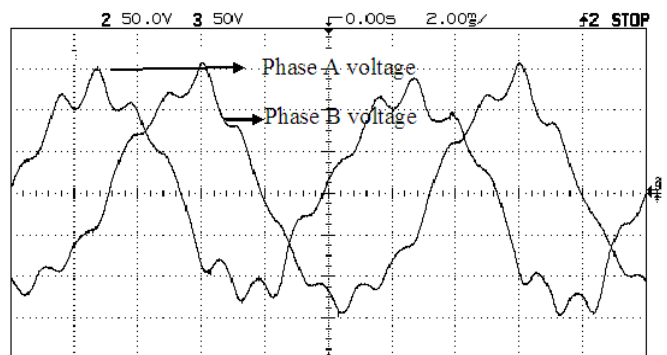


Fig. 11 Terminal Per Phase Voltage for two phases ($I_f=2A$, 1500 r.p.m., voltage Scale=10:1)

Fig. 12 shows the terminal voltage per phase for the three phases with flux barrier rotor when loaded with R-load with a delta connected capacitor bank is connected in parallel with the load.

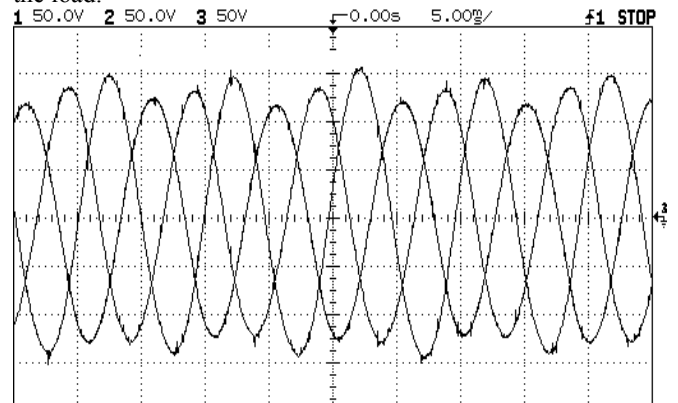


Fig. 12. Terminal Per Phase Voltage for three phases ($I_f=2A$, 1500 r.p.m., voltage Scale=10:1, $C=10$ microfarad (per phase))

From this figure, one can see that the waveforms become approximately pure sine waves and there is 120 degree phase shift between any two subsequent phases. Fig. 13 shows the terminal voltage per phase and the per phase current with R-load with a delta connected capacitor bank is connected in parallel with the load.

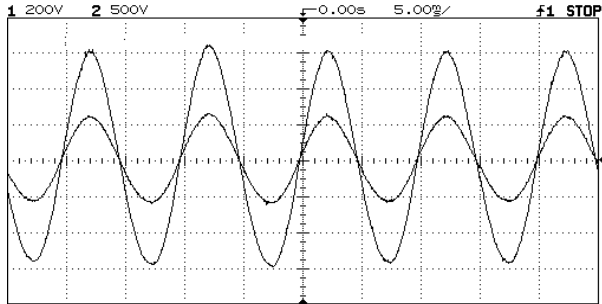


Fig. 13 Terminal Per Phase Voltage & phase Current ($I_f=2A$, 1500 r.p.m., voltage Scale=10:1, $C=12$ microfarad (per phase))

Figs. 14&15 show the loading characteristics with flux barrier rotor when loaded with R-load and with RL-load. From these figures, one can see that the obtained characteristics are very close to the conventional synchronous machine. It is expected that a better performance will be obtained with changes in stator design to accommodate more field conductors.

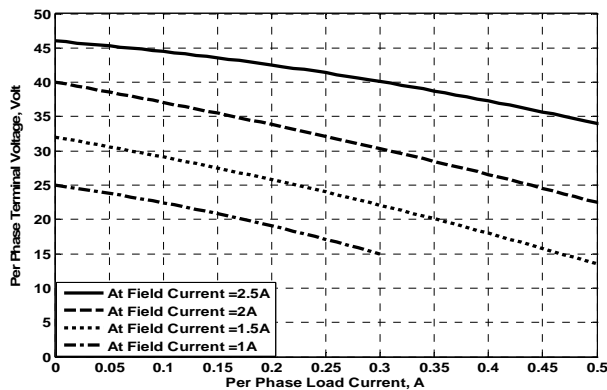


Fig. 14 Loading Characteristics with R-Load at 1500 R.P.M.

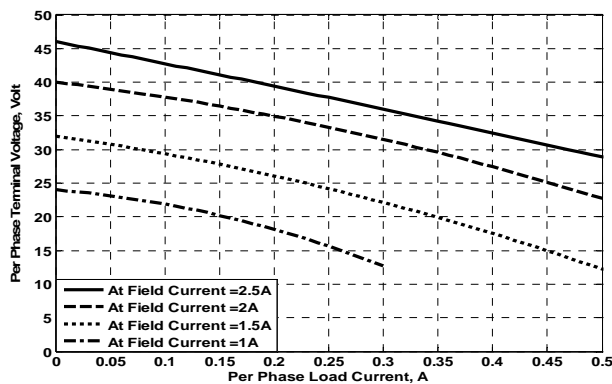


Fig. 15 Loading Characteristics with RL-Load at 1500 R.P.M, power factor=0.4

Fig. 16 shows the torque variation versus time as calculated by using the machine model. For more details about the machine model see [2]. Also, one can see that the torque contains quietly high torque ripples. As stated before, these ripples may be reduced by providing pole skewing and using a laminated rotor.

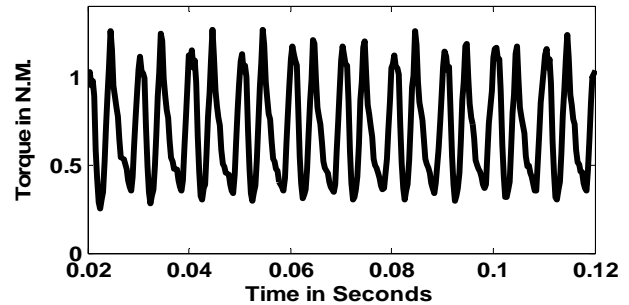


Fig. 16 Electromagnetic Torque as Calculated from Machine Model at 1500 R.P.M.

VIII. DESIGN OF A 1.6 KVA DSWBA

By using the equations derived in the above sections and by using a finite element tool a 1.6 KVA brushless generator was designed with the following design data:

- Machine rating=1.6 KVA.
- Machine rated voltage=220 volts/phase.
- Stator bore diameter (D) =20 cm.
- Axial length (L) =11 cm.
- Air gap length= 1 mm.
- Stator slots (S) =36 slots.
- Pole arc coefficient=0.63
- No. of field conductors/slot=250 cond.
- Field current= 4 A.
- Generating conductors/slot= 40 cond.

By using the finite element tool and the following MATLAB SIMULINK model the following characteristics has been obtained.

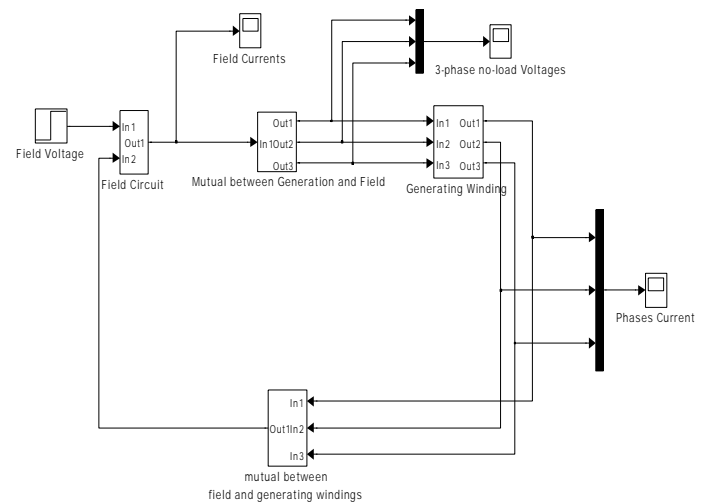


Fig. 17 DSWBA SIMULINK Model, Ref. [2]

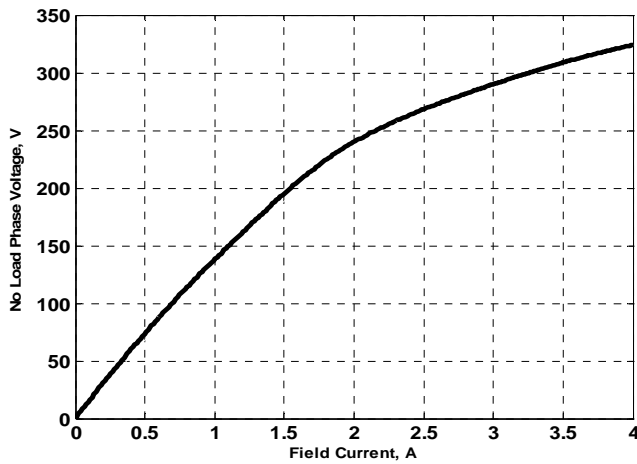


Fig. 18 No Load Characteristic of the Designed Machine, 1500 R.P.M.

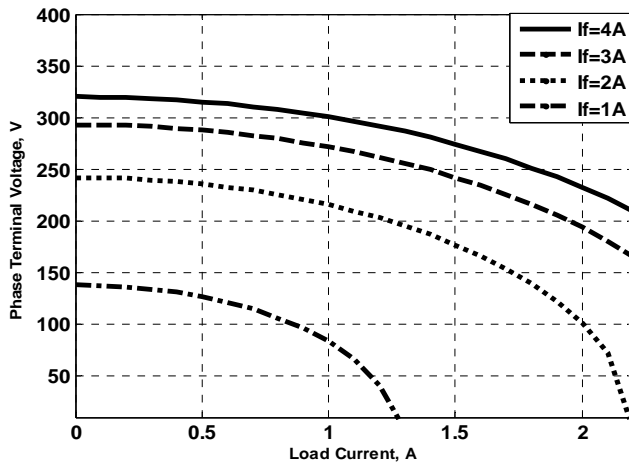


Fig. 19 Terminal Voltage versus Load Current of the Designed Machine, R-Load, 1500 R.P.M.

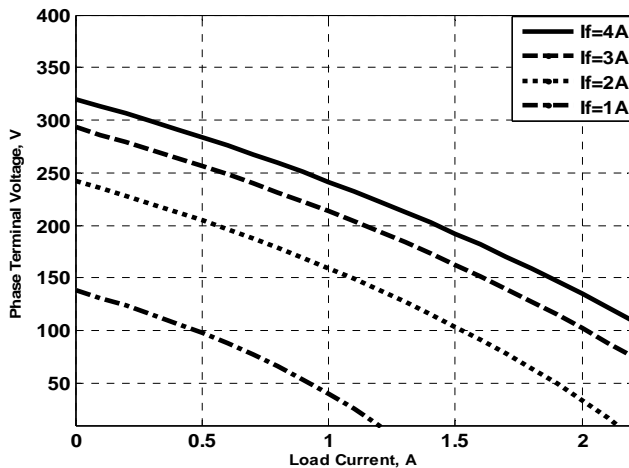


Fig. 20 Terminal Voltage versus Load Current of the Designed Machine, RL-Load, power factor=0.8, 1500 R.P.M.

From the above figures, it can be shown that the proposed technique for designing the DSWBA is valid and can be used for designing such these machines of any power rating.

IX. CONCLUSION

A design technique for a DSWBA has been presented. A 1.6 KVA generator has been designed using the presented technique. The machine performance has been studied by building a prototype using a standard stator of a 1 hp induction motor. Also, the performance of the 1.6 KVA has been studied (theoretically). The proposed generator is a reliable and can be used in remote areas.

ACKNOWLEDGMENT

The authors would like to thank Prof. Dr. Anwar Abdel Latif Hassaneien and Dr. Tamer Fetouh Abdel Ghany for their help and support.

REFERENCES

- [1] Hocine Amimeur et al "A Sliding Mode Control Associated to the Field-Oriented Control of Dual-Stator Induction Motor Drives", Jee Journal, Vol. 10, 2010.
- [2] M. El-Shanawany, S.M.R. Tahoun and M. Ezzat, "A Dual Stator Winding-Mixed Pole Brushless Synchronous Generator (Design, Performance Analysis & Modeling)", Proceedings of the POWRM Conference, Japan, PP. 159-165, 4-6 Oct. 2010.
- [3] M. G. Javonovic, R. E. Betz, and J.Yu "The use of doubly fed reluctance machines for large pumps and wind turbines", IEEE, 2001.
- [4] Y. Liao, L. Zhen and L. Xu, "Design of a doubly-fed reluctance motor for adjustable speed drives", Proceedings of the IAS Annual Meeting, Vol. 1, PP. 305-312, Oct. 1994.
- [5] G. Javonovic, "A Comparative Study of Control Strategies for Performance Optimisation of Brushless Doubly-Fed Reluctance Machines", J.Electrical Systems, 2-4 (2006), PP. 208-225.
- [6] R. Betz and M. Gavonovic, "Control aspects of brushless doubly fed reluctance machines", Proceedings of the European Power Electronics Conference (EPE'99), Sept. 1999.
- [7] Feng Liang, Longya Xu and T.A. Lipo "d-q Analysis of a Variable Speed Doubly AC Excited Motor", Electric Machines and Power Systems, Vol. 19, pp. 125-138, March 1991.
- [8] R. Betz and M. Gavonovic, "Introduction to Brushless Doubly Fed Reluctance Machines- The Basic Equations", Tech. Rep. EE0023, Department of Electrical Engineering, University of Newcastle, Australia, April 1998.
- [9] R. Betz and M. Gavonovic, "Comparison of the brushless doubly fed reluctance machine and the synchronous reluctance machine", Tech. Rep. EE0023, Department of Electrical Engineering, University of Newcastle, Australia, October 1998.
- [10] R. E. Betz, M. G. Javonovic, "Introduction to the Space Vector Modelling of the Brushless Doubly-Fed Reluctance Machine", Electric Power Components and Systems, 31:729-755, 2003.
- [11] E. M. Schulz and R. Betz, "Optimal Rotor Design of Brushless Doubly Fed Reluctance Machines", IEEE, PP. 256-261, 2003.
- [12] A. R. W. Broadway, L. Burbridge, "Self-Cascaded Machine: a Low Speed Motor or High Frequency Brushless Alternator", Proc. IEE, Vol. 117, July 1970, PP. 1277-1290.

NOMENCLATURE

If	Field Current.
I _{ph}	Phase Current.
K _{wf}	Field winding factor.
P ₂	Number of field winding poles (6-pole).
P _r	Number of rotor poles (4-pole).
S	Number of stator slots.
Z _f	Number of field conductors per slot.
y	Rotor pole arc/pole pitch ratio.